

Subband dispersion of holes in AlAs/In_{0.10}Ga_{0.90}As/AlAs strained-layer quantum wells measured by resonant magnetotunneling

S. Y. Lin, A. Zaslavsky,^{a)} K. Hirakawa, and D. C. Tsui
Princeton University, Department of Electrical Engineering, Princeton, New Jersey 08544

J. F. Klem
Sandia National Laboratories, Albuquerque, New Mexico 87185

(Received 31 October 1991; accepted for publication 16 November 1991)

Magnetotunneling of holes through the double-barrier AlAs/In_{0.10}Ga_{0.90}As strained-layer structure is investigated with magnetic fields up to 23 T to determine the in-plane dispersion of the two-dimensional subbands in the In_{0.10}Ga_{0.90}As quantum well. Mass reversal, nonparabolicity, anticrossing, and anisotropy are observed. The lack of electronlike dispersion in the lowest-energy light-hole subband is attributed to the large biaxial compressional strain in the In_{0.10}Ga_{0.90}As, which suppresses the mixing of heavy and light-hole states even at finite in-plane wave vectors.

Charge transport through a double-barrier resonant tunneling structure (DBRTS) depends explicitly on the energy levels of the heterostructure,^{1,2} and therefore can give direct information about the energy structure of the two-dimensional (2D) subbands in the quantum well. When a strong magnetic field B is applied parallel to the tunneling direction, it induces oscillatory features in the current-voltage I - V characteristic. These features arise from resonant tunneling into the Landau levels in the quantum well and thus provide a way to determine the effective mass of the carriers.^{3,4} When B is applied transverse to the tunneling direction (B_{\perp}), the charge carriers will acquire a transverse momentum ΔK_{\perp} in the course of tunneling through the emitter barrier. This additional transverse momentum induces a shift in the voltage position V_p of the resonance peak in the I - V .⁵ Since the shift in V_p and the change in K_{\perp} are directly related to the subband energy-momentum (E - K_{\perp}) dispersion, resonant magnetotunneling can be a tool to probe the subband in-plane dispersion. It is particularly useful for studying complex energy structures since it probes specific values of the K_{\perp} , not an average over K space.

The application of this technique to study the complex valence-band (VB) dispersion has recently been reported by Hayden *et al.*⁶ in p -type AlAs/GaAs/AlAs and by Gennser *et al.*⁷ in p -type Si/Si_{1-x}Ge_x/Si. We wish to report in this letter the first magnetotunneling measurements on p -type AlAs/In_{0.10}Ga_{0.90}As/AlAs strained-layer structures and the in-plane dispersion of the VB determined with B_{\perp} up to 23 T. The large biaxial strain in the In_{0.10}Ga_{0.90}As layer splits the fourfold degenerate VB edge ($K=0$) and modifies the energy structure of the strain split-off subbands.⁸ For $K_{\perp} < 2 \times 10^8 \text{ m}^{-1}$, we observe a strong in-plane dispersion (i.e., light effective mass) for the heavy-hole (HH) ground subband of the In_{0.10}Ga_{0.90}As well and about three times weaker dispersion (i.e., heavy effective mass) for the light-hole (LH) ground subband. Surprisingly, we did not observe the electronlike states in the LH₀

subband of the strained In_{0.10}Ga_{0.90}As well for K_{\perp} up to $5 \times 10^8 \text{ m}^{-1}$. This observation is contrary to the theoretically predicted and recently reported LH₀ subband dispersion in the lattice-matched Al_xGa_{1-x}As/GaAs structures. Our result is a direct consequence of the large biaxial compressive strain in the In_{0.10}Ga_{0.90}As layer which effectively decouples the HH-LH bands even at finite K_{\perp} . The observation of a light in-plane mass for the HH₀ subband and a heavy in-plane mass for the LH₀ subband at small K_{\perp} is also consistent with this effective decoupling of HH-LH bands by the strain. In addition, large in-plane anisotropy is observed and estimated to be $\approx 20\%$ for the HH₀ and LH₀ subbands in the In_{0.10}Ga_{0.90}As well.

Two DBRTS device structures, grown by molecular-beam epitaxy on a (001) p^+ -GaAs substrate, were investigated. The active region of device 1 consists of (1) 0.2 μm of GaAs, Be doped to $2 \times 10^{18}/\text{cm}^3$, (2) 0.1 μm of GaAs, Be doped to $1 \times 10^{18}/\text{cm}^3$, (3) 0.1 μm of GaAs, Be doped to $5 \times 10^{17}/\text{cm}^3$, (4) 500 \AA of undoped GaAs, (5) 60 \AA of undoped AlAs barrier, (6) $W = 42 \text{\AA}$ of undoped In_{0.10}Ga_{0.90}As well, (7) 70 \AA of undoped AlAs barrier, (8) 500 \AA of undoped GaAs, (9) 0.1 μm of GaAs, Be doped to $5 \times 10^{17}/\text{cm}^3$, (10) 0.1 μm of GaAs, Be doped to $1 \times 10^{18}/\text{cm}^3$, and (11) 0.3 μm of GaAs, Be doped to $2 \times 10^{18}/\text{cm}^3$. Device 2 differs only in the quantum-well thickness, $W = 34 \text{\AA}$. The undoped spacer layers outside the barriers are intended to prevent dopant diffusion into the quantum well. The barrier asymmetry is designed to prevent significant charge buildup in the well at the forward bias.⁵ The devices were defined by the $45 \times 45\text{-}\mu\text{m}^2$ contact pads of Au-Zn-Au square dots which were used as a mask for the mesa etching. Ohmic contacts were formed by alloying at 400 $^{\circ}\text{C}$ in hydrogen ambient. The magnetotunneling measurements were performed at 4.2 K with B_{\perp} to 9 T in a superconducting magnet and to 23 T in a Bitter magnet. The sample was mounted in a rotating sample holder; its I - V and the derivatives were measured using conventional ac lock-in technique.

The I - V of two DBRTS devices in forward bias at $B=0$ are shown as the lower two traces in Fig. 1. The d^2I/dV^2 - V for device 1 ($W=42 \text{\AA}$) is shown as the top

^{a)}Presently at IBM T. J. Watson Research Center, P. O. Box 218, Yorktown Height, NY 10598.

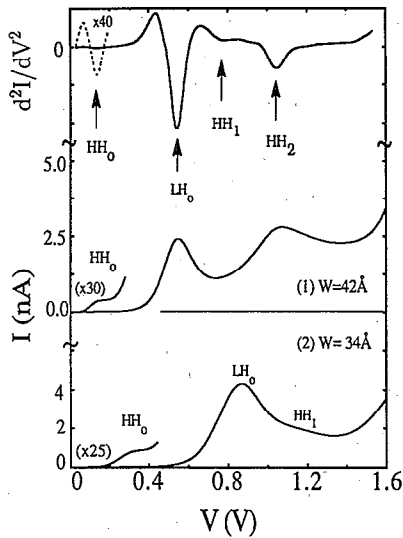


FIG. 1. I - V characteristics of two AlAs/In_{0.10}Ga_{0.90}As/AlAs DBRTS devices at 4.2 K. W is the thickness of the In_{0.10}Ga_{0.90}As layer. The lower two traces are I - V . The top trace is the d^2I/dV^2 - V of device with $W=42$ Å.

trace. In device 1, the tunneling current rises at $V \approx 60$ mV, showing a weak but clear shoulder at ≈ 150 mV. At higher biases, two resonance peaks are seen at $V = 553$ and 1080 mV. In the d^2I/dV^2 - V , the two strongest minima labeled LH₀ and HH₂ correspond to the two resonance peaks in the I - V . The HH₀ minimum at $V=145$ mV is the ground subband resonance. In addition, a weak minimum, not apparent in the I - V , is resolved at $V = 780$ mV and is labeled HH₁. For device 2, which has a narrower well width ($W = 34$ Å), all the resonances are shifted to higher biases. The HH₀ and the LH₀ resonances are observed at $V = 306$ and 820 mV, respectively, and the HH₁ resonance is discernible in the I - V as a shoulder at $V \approx 1.2$ V. Since both the quantum confinement and the biaxial compressive strain in the well act to split the HH-LH subbands at Γ ($K=0$) and push the HH subband upward in energy, the HH subband must be the uppermost valence-band states in the In_{0.10}Ga_{0.90}As well. We therefore assign the HH₀ resonance to tunneling of holes into the HH ground subband. Moreover, the current level at the LH₀ resonance is about two orders of magnitude higher than that at the HH₀ resonance in both devices. Since the tunneling probability of holes into the LH ground subband is expected to be orders of magnitude larger than that into the HH ground subband,⁹ we assign the LH₀ resonance peak to the LH ground subband. The HH₁ and HH₂ resonances are assigned to the first and second HH excited subbands, respectively. This assignment is based on an energy-level calculation using the band parameters deduced from the HH₀ and LH₀ resonances and assuming a band offset of 480 mV (Ref. 10) for HH at the AlAs/In_{0.10}Ga_{0.90}As heterojunction.

The application of B_{\perp} shifts the voltage position V_p of the resonances. We have investigated to 23 T this shift of the HH₀ and LH₀ resonances in both devices and plotted

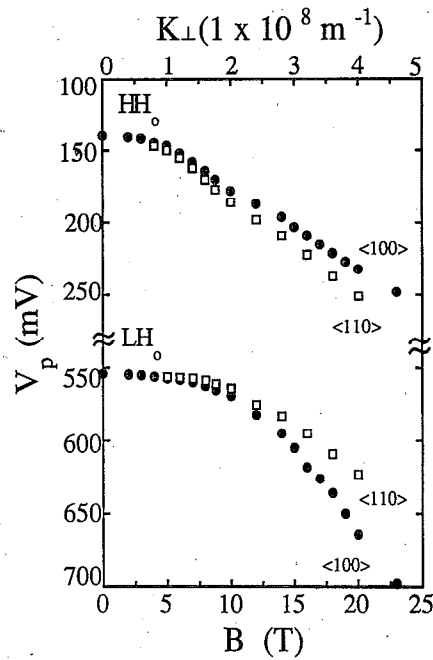


FIG. 2. Voltage position V_p of the HH₀ and LH₀ resonance peak as a function of B_{\perp} , applied along a $\langle 100 \rangle$ direction (closed dots) and a $\langle 110 \rangle$ direction (open squares) in the plane of the AlAs/In_{0.10}Ga_{0.90}As interface.

our data from device 1 as V_p vs B_{\perp} in Fig. 2. The solid dots are the data taken with B_{\perp} applied along a $\langle 100 \rangle$ axis of the sample and the open squares are with B_{\perp} along a $\langle 110 \rangle$ axis. The shift in V_p arises from the change in the in-plane momentum, ΔK_{\perp} , induced by B_{\perp} . If we take B_{\perp} to be along x axis and the tunnel current along z -axis, a hole in the emitter state (E, K_x, K_y) will tunnel elastically into the subband state ($E, K_x, K_y - \Delta K_y$) of the well. ΔK_y is given by

$$\Delta K_y = eB_{\perp} \langle z \rangle / \hbar, \quad (1)$$

where $\langle z \rangle$ is the average hole traversal distance. Since the energy is conserved in the tunneling process, any gain in kinetic energy due to the change in ΔK_y must be supplied by a change in bias and thus cause a shift in V_p . Therefore, the plot of V_p vs B_{\perp} in Fig. 2 is a display of the subband dispersion in the quantum well, and the difference in V_p for different orientations of B_{\perp} in the plane of the interface is a direct measure of the subband anisotropy. The corresponding K_{\perp} , calculated from Eq. (1) using $\langle z \rangle = 125$ Å for the device,¹¹ is shown in the upper horizontal axis.

We first neglect the anisotropy and concentrate on the dispersion for K_{\perp} along $\langle 100 \rangle$. It is clear from the data that for small K_{\perp} ($B_{\perp} \leq 10$ T, corresponding to $K_{\perp} < 2 \times 10^8$ m⁻¹) the HH₀ subband is much more dispersive than the LH₀ subband, as anticipated from the so-called diagonal approximation (which neglects mixing of HH and LH states) that the HH subband should display a light in-plane mass and the LH subband should display a heavy in-plane mass.¹² This valence-band mass reversal effect is well known in strained material^{8,13} and has been a main reason for the interest in using p -type In_xGa_{1-x}As strained-layer structure for high-speed electronic applications.¹⁴ For

$B_1 > 10$ T, in the large K_1 limit, the HH_0 subband becomes nonparabolic, showing an almost linear dispersion. Such a high degree of nonparabolicity in the HH_0 subband has also been deduced from magneto-luminescence experiments recently by Jones *et al.*¹⁵ The LH_0 subband, on the other hand, takes on the lighter mass dispersion in this limit, suggestive of the anticrossinglike feature seen in several theoretical calculations.^{12,16-18} This feature arises from mixing of the HH and LH states at finite K_1 , when the off-diagonal terms are included in the valence-band Hamiltonian. We must also emphasize that the dispersion of our LH_0 subband is strictly holelike and there is no indication in the data of the electronlike dispersion (i.e., having camel-back shape or negative hole masses) predicted in these calculations. This may at first appear surprising in that electronlike dispersion has recently been seen in the lattice-matched $\text{GaAs}/\text{Al}_x\text{Ga}_{1-x}\text{As}$ quantum-well structure.⁶ Again, the electronlike dispersion results from the strong mixing of HH and LH hole states at finite K_1 . In our strained-layer structure, the strain induced splitting is ≈ 25 meV, sufficiently large to decouple the HH and LH states to make the mixing due to quantum confinement negligible and, as a result, we do not expect the LH_0 subband to display the electronlike dispersion.

Finally, we have investigated the subband anisotropy (or warping) by rotating B in the interface plane. We find that both subbands are essentially isotropic for $B \leq 5$ T ($K_1 < 1 \times 10^8 \text{ m}^{-1}$). The anisotropy, which is expected when warping of the bulk valence bands is taken into account, is clearly resolved at ≈ 10 T for $K_1 \approx 2 \times 10^8 \text{ m}^{-1}$ and increases to $\approx 20\%$ at $K_1 \approx 4 \times 10^8 \text{ m}^{-1}$ or $B_1 \approx 20$ T (see Fig. 2). Similar anisotropy of comparable magnitude has recently been observed in the $\text{Si}/\text{Si}_{1-x}\text{Ge}_x$ strained-layer structure by Gennser *et al.*⁷ However, in the lattice-matched $\text{GaAs}/\text{Al}_x\text{Ga}_{1-x}\text{As}$ structure, Hayden *et al.*⁶ found only a very small anisotropy. Thus the large anisotropy observed in our samples and in the $\text{Si}/\text{Si}_{1-x}\text{Ge}_x$ must also be due to the large biaxial strain that alters the band mixing.¹⁹

We thank Dr. R. Du for assistance and one of us (K.H.) would like to thank the Japan Society for Promotion of Science for financial support. Part of this work was carried out at the France Bitter National Magnet Laboratory, which is funded by National Science Foundation. The work at Princeton University is supported by the AFOSR and at Sandia by the U. S. Department of Energy under Contract No. DE-AC04-76DP00789.

- ¹L. L. Chang, L. Esaki, and R. Tsu, *Appl. Phys. Lett.* **24**, 593 (1974).
- ²E. E. Mendez, W. I. Wang, B. Ricco, and L. Esaki, *Appl. Phys. Lett.* **47**, 415 (1985).
- ³E. E. Mendez, L. Esaki, and W. I. Wang, *Phys. Rev. B* **33**, 2893 (1986).
- ⁴V. J. Goldman, D. C. Tsui, and J. E. Cunningham, *Phys. Rev. B* **35**, 9387 (1987).
- ⁵A. Zaslavsky, Y. P. Li, D. C. Tsui, M. Santos, and M. Shayegan, *Phys. Rev. B* **42**, 1374 (1990).
- ⁶R. K. Hayden, D. K. Maude, L. Eaves, E. C. Valadares, M. Henini, F. W. Sheard, O. H. Hughes, J. C. Portal, and L. Cury, *Phys. Rev. Lett.* **66**, 1749 (1991).
- ⁷U. Gennser, V. P. Kesan, D. A. Syphers, T. P. Smith III, S. S. Iyer, and E. S. Yang (private communication).
- ⁸G. C. Osbourn, *J. Vac. Sci. Technol. B* **1**, 379 (1983); *Superlatt. Microstruct.* **1**, 223 (1985).
- ⁹R. Wessel and M. Altarelli, *Phys. Rev. B* **39**, 12802 (1989).
- ¹⁰W. I. Wang and F. Stern, *J. Vac. Sci. Technol. B* **3**, 1280 (1985); G. Ji, D. Huang, U. K. Reddy, T. S. Henderson, R. Houdre, and H. Morkoc, *J. Appl. Phys.* **62** 3366 (1987).
- ¹¹ $\langle z \rangle$ is approximated by $\lambda + b_1 + W/2$, where λ is the emitter screening length and b_1 is the thickness of the emitter barrier.
- ¹²G. Bastard and J. A. Brum, *IEEE J. Quantum Electron.* **QE-22**, 1625 (1986).
- ¹³J. C. Hensel and G. Feher, *Phys. Rev. Lett.* **5**, 307 (1960).
- ¹⁴T. J. Drummond, T. E. Zipperian, I. J. Fritz, J. E. Schirber, and T. A. Plut, *Appl. Phys. Lett.* **49**, 461 (1986).
- ¹⁵E. D. Jones, S. K. Lyo, I. J. Fritz, J. F. Klem, J. E. Schirber, C. P. Tiggs, and T. J. Drummond, *Appl. Phys. Lett.* **54**, 2227 (1989).
- ¹⁶M. Altarelli, U. Ekenberg, and A. Fasolino, *Phys. Rev. B* **32**, 5138 (1985).
- ¹⁷L. C. Andreani, A. Pasquarello, and F. Bassani, *Phys. Rev. B* **36**, 5887 (1987).
- ¹⁸T. Ando, *J. Phys. Soc. Jpn.* **54**, 1528 (1985).
- ¹⁹G. D. Sanders and Y.-C. Chang, *Phys. Rev. B* **32**, 4282 (1985).